Water Research 173 (2020) 115575

Contents lists available at ScienceDirect

Water Research

journal homepage: www.elsevier.com/locate/watres

Nitrogen removal as nitrous oxide for energy recovery: Increased process stability and high nitrous yields at short hydraulic residence times

Zhiyue Wang [a, b], Sung-Geun Woo [a, b], Yinuo Yao [a, b], Hai-Hsuan Cheng [c], Yi-Ju Wu [c], Craig S. Criddle [a, b, *]

[a] Department of Civil and Environmental Engineering, Stanford University, Stanford, CA, USA
[b] U.S. National Science Foundation Engineering Research Center for Re-inventing the Nation's Urban Water Infrastructure (ReNUWIt), USA
[c] Department of Environmental Engineering, National Cheng Kung University, Tainan, Taiwan

ARTICLE INFO

Article history:
Received 17 October 2019
Received in revised form
29 January 2020
Accepted 30 January 2020
Available online 4 February 2020

Keywords:
Anaerobic digester centrate
Denitritation
Nitrous oxide
Polyhydroxyalkanoate
Short-cut nitrogen removal
Wastewater

ABSTRACT

The Coupled Aerobic-anoxic Nitrous Decomposition Operation (CANDO) is a two-stage process for nitrogen removal and resource recovery: in the first, ammonia is oxidized to nitrite in an aerobic bioreactor; in the second, oxidation of polyhydroxyalkanoate (PHA) drives reduction of nitrite to nitrous oxide (N_2O) which is stripped for use as a biogas oxidant. Because ammonia oxidation is well-studied, tests of CANDO to date have focused on N_2O production in anaerobic/anoxic sequencing batch reactors. In these reactors, nitrogen is provided as nitrite; PHA is produced from acetate or other dissolved COD, and PHA oxidation is coupled to N_2O production from nitrite. In a pilot-scale study, N_2O recovery was affected by COD/N ratio, total cycle time, and relative time periods for PHA synthesis and N_2O production. In follow-up bench-scale studies, different reactor cycle times were used to investigate these operational parameters. Increasing COD/N ratio improved nitrite removal and increased biosolids concentration. Shortening the anaerobic phase prevented fermentation of PHA and improved its utilization. Efficient PHA synthesis and utilization in the anaerobic phase correlated with high N_2O production in the anoxic phase. Shortening the anoxic phase prevented reduction of N_2O to N_2. By shortening both phases, total cycle time was reduced from 24 to 12 h. This optimized operation enabled increased biomass concentrations, increased N_2O yields (from 71 to 87%), increased N loading rates (from 0.1 to 0.25 kg N/m^3-d), and shorter hydraulic residence times (from 10 to 2 days). Long-term changes in operational performance for the different bioreactor systems tested were generally similar despite significant differences in microbial community structure. Long-term operation at short anaerobic phases selected for a glycogen-accumulating community dominated by a *Defluviicoccus*-related strain.

1. Introduction

As a result of anthropogenic nitrogen fixation, reactive nitrogen species entering the global nitrogen cycle has doubled in the last century (Fowler et al., 2013). Release of reactive nitrogen from wastewater into natural water bodies can stimulate eutrophication and create oxygen-depleted zones (Selman et al., 2008). Conventional nitrogen removal processes need significant energy input for aeration, require reducing power, and generate large amount of waste biosolids for disposal. These issues can be addressed through shortcut nitrogen removal processes in which ammonium is oxidized to nitrite, and nitrite is reduced to dinitrogen gas (N_2) with either heterotrophic or autotrophic denitrifiers. Adopting the nitrogen cycle nomenclature of Weißbach et al., 2017, nitritation accompanied by heterotrophic denitritation to N_2 can decrease aeration requirements by 25% and demand for organic carbon (reducing equivalents) by 40% (Hellinga et al., 1998). Autotrophic denitritation, such as Anammox, can further decrease demand for organic carbon to zero (Lackner et al., 2014). Due to process control issues, however,

* Corresponding author. Jerry Yang & Akiko Yamazaki Building, 473 Via Ortega, Room 161, Stanford, CA, 94305, USA.
E-mail address: criddle@stanford.edu (C.S. Criddle).

https://doi.org/10.1016/j.watres.2020.115575
0043-1354/

shortcut nitrogen removal processes can release more nitrous oxide (N_2O) than conventional processes (Massara et al., 2017).

The Coupled Aerobic-anoxic Nitrous Decomposition Operation (CANDO) was developed to remove nitrogen from wastewater and produce N_2O in a controlled manner for energy recovery (Scherson et al., 2013, 2014). The process involves two reactors: in the first, high concentrations of ammonia, typically present in anaerobic digestate, are oxidized to nitrite; in the second, nitrite is reduced to N_2O (nitrous denitritation). Advantages of CANDO over conventional nitrogen removal include: (1) a 60% decrease in demand for organic electron donor, whether it be wastewater organic matter used to produce methane or purchased organic substrate, such as methanol; (2) limiting nitrite reduction to N_2O, thereby decreasing biosolids production by 60% as compared to nitrate reduction to N_2 (Gao et al., 2014) and reducing associated costs of transport and disposal, and (3) use of N_2O as an oxidant for combustion of biogas methane yields more heat ($\Delta H_c = -1219$ kJ/mol CH_4) than combustion with oxygen ($\Delta H_c = -890$ kJ/mol CH_4) increasing by 6–7% the power output achieved per unit of methane oxidized in a combustion engine (Scherson et al., 2014).

The source of carbon used to provide electrons for nitrous denitritation is flexible. A research team at the Technical University of Munich used multiple dosages of primary effluent as the carbon source for nitrous denitritation (Weißbach et al., 2018b). Another team at Northwestern University used a mixture of acetate and propionate to enrich for denitrifying polyphosphate accumulating organisms, enabling simultaneous nitrogen and phosphorus removal (Gao et al., 2017). Promising results from bench-scale studies led to a CANDO scale-up, aiming to (1) evaluate process stability, (2) identify potential interferences, and (3) optimize process control under real-world operational conditions. In the present study, we document the performance of a pilot-scale nitrous denitritation reactor treating nitrified anaerobic digester centrate (~1 g NO_2–N/L), produced by a pilot-scale nitritation reactor treating anaerobic digester centrate (~1.5 g TKN/L). On occasion, the nitritation reactor was subject to upsets that carried over to the nitrous denitritation reactor and affected its performance. During these upset periods, a surrogate nitrified centrate was fed to the nitrous denitritation reactor until process control was re-established. After completion of the pilot study, follow-up bench-scale studies were initiated to improve and optimize process performance. These studies gave deeper insight into process operations and enabled significant improvements in process loading and operational stability.

2. Material and methods

2.1. Pilot-scale reactor setup and operation

A sequencing batch reactor (SBR) with a volume of 6 m^3 and a total liquid volume of 1.5 m^3 was established at Delta Diablo wastewater treatment plant (Antioch, CA, USA). The reactor was fed a stock solution of sodium acetate and acetic acid (pH = 4.0, COD = 4.5 g/L), and effluent from a nitritation reactor treated anaerobic digester centrate (East Bay Municipal Utility District and Project Partners, 2017) containing ~1.1 g NO_2–N/L or a surrogate nitrified centrate containing 1 g NO_2–N/L (Scherson et al., 2013). Reactor pH was maintained at 8.0 by automated addition of hydrochloric acid based on readings from a self-cleaning flat pH probe (Cole-Parmer, IL, USA). In-situ probes were installed to monitor concentrations of dissolved reactive nitrogen species. A UV–vis spectrophotometer (S:CAN uv:lyser UV, Austria) was used to monitor nitrite and nitrate. An industrial Clark-type sensor (Unisense, Denmark) was used for dissolved N_2O monitoring.

The pilot-scale nitrous denitritation SBR was inoculated with 150 L (10% v/v) of returned activated sludge from Delta Diablo then operated for 315 days. Acetate was added as a pulse at the start of each operational cycle to initiate the anaerobic phase. Nitrite was added as a pulse at the end of the anaerobic phase to initiate the anoxic phase, and air stripping enabled recovery of dissolved N_2O at the end of each cycle (Fig. 1). During start-up, the reactor was operated for 60 days without settling to select for N_2O-producing microorganisms (Table S1). The initial COD/N input ratio (g COD as acetate/g N as nitrite) was set at five (150 mg COD/L and 30 mg N/L). To concentrate biomass, a settle/decant step was added before discharge of effluent. The cycle time was changed to 24 h, and the COD/N input ratio was decreased to 3. Stable operation began on day 164 (Period I), and the aeration period was extended to 3 h. In Period II, the duration of the anaerobic phase was reduced to 7 h and remained at that level for the duration of the experiment.

The pilot reactor experienced two significant perturbations due to upsets in the upstream nitritation reactor. On days 61–72 and 107–113, inefficient upstream nitritation resulted in high levels of ammonium and low concentrations of nitrite in the influent to the nitrous denitritation SBR. On days 251–257, a process control issue in the upstream nitritation reactor resulted in high concentrations of nitrate in the influent to the nitrous denitritation SBR. When these upset periods were detected, a surrogate nitrified centrate was fed to the denitritation reactor in lieu of influent from the nitritation reactor. This switch in the influent feed enabled

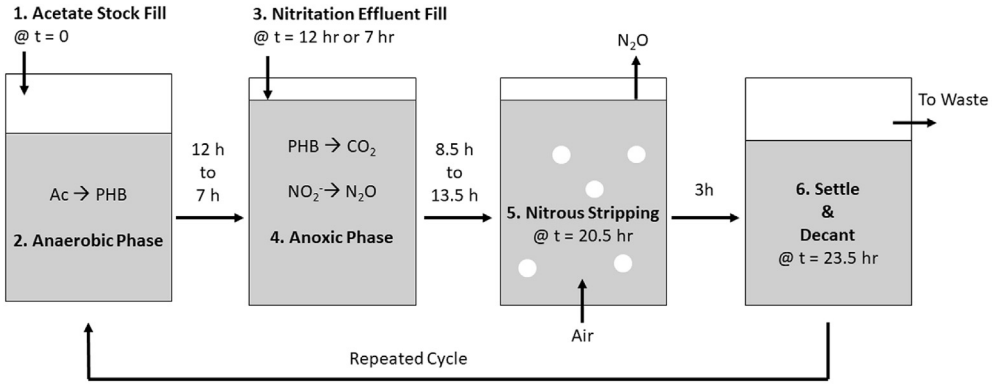

Fig. 1. Schematic diagram for the operation of the pilot-scale nitrous denitritation SBR. Duration of the anaerobic phase was initially 12 h then switched to 7 h. Duration of the anoxic phase was initially 8.5 h then switched to 13.5 h.

operational continuity while the nitritation reactor recovered from process upsets.

2.2. Bench-scale reactor setup and operation

To explore the effects of different operational and design variables, two 5-L bench-scale nitrous denitritation SBRs (SBR-1 and SBR-2), each with a total liquid volume of 4 L, were fed nitrite-rich effluent from a bench-scale nitritation SBR that in turn was fed anaerobic digester centrate from Delta Diablo. The nitrite-rich effluent contained 1100 mg/L NO_2^--N, 60 mg/L NH_4^+-N, 30 mg/L NO_3^--N and a soluble COD of 200 mg/L. The operational cycle was similar to that of the pilot-scale reactor, with a 21.5-h reaction phase, 2-h stripping phase, 20 min settle and 10 min of decant. During the react phase, SBR-1 had a 12-h anaerobic phase and a 9.5-h anoxic phase; SBR-2 had an 8-h anaerobic phase and a 13.5-h anoxic phase. Both reactors were operated at an HRT of 4 days and a solid retention time (SRT) of 60 days. A solution of sodium acetate and acetic acid (3 g COD/L, pH = 5.0) was used as the carbon source for denitritation. The pH of the both reactors was maintained at 7.5 by automatic addition of 1 M HCl. The same decoupled feeding strategy as the pilot-scale SBR for acetate and nitrite was used to enrich for N_2O-producing bacteria in the bench-scale reactors.

2.3. Chemical analysis of water and biomass samples

Water samples from the pilot-scale reactor were filtered through 0.45 μm Nylon filters and stored at −20 °C before analysis. For the bench-scale studies, water samples were filtered and stored at 4 °C before analysis. Standard Methods (Rice et al., 2017) were used for analysis of ammonia, nitrite, nitrate, mixed liquor total suspended solids (MLTSS), mixed liquor volatile suspended solids (MLVSS), soluble chemical oxygen demand (sCOD) and total chemical oxygen demand (tCOD). Poly-3-hydroxybutyrate (PHB) and poly(3-hydroxybutyrate-co-3-hydroxyvalerate) (PHBV) were extracted from lyophilized biomass, depolymerized, methylated and measured on an Agilent 6890N gas chromatography with flame ionization detector and a HP-5 column (Agilent, CA, USA) as previously described (Myung et al., 2015). Concentrations of measured PHA monomers were denoted as 3-hydroxybutyrate (HB) and 3-hydroxyvalerate (HV). Headspace gaseous samples were collected with vacuum serum bottles and analyzed on a Varian 3800 gas chromatography (Agilent, CA, USA) with a Porapak Q column, a 5 Å molecular sieve column and a thermal conductivity detector (Scherson et al., 2014). Total carbohydrate content of lyophilized biomass samples was determined by the anthrone method (Gerhardt et al., 1994).

2.4. DNA extraction and illumina sequencing

Genomic DNA was extracted from 11 pilot-scale reactor biomass samples and 5 bench-scale SBR-2 biomass samples using the FastDNA Spin Kit for soil (MP Biomedicals, Solon, OH) per manufacturer's protocol. A PCR amplification targeting the V3 and V4 region of bacterial 16S rRNA gene was performed using forward primer S-D-Bact-0341-b-S-17 (5′- CCTACGGGNGGCWGCAG) and reverse primer S-D-Bact-0785-a-A-21 (5′- GGACTACHVGGGTATCTAATCC) (Klindworth et al., 2013). A 25-μL PCR reaction was carried out using 0.25 μM of each primer, 2X Fail-Safe PCR buffer F (Epicentre, Madison, WI), 1.25 units of AccuPrime™ Taq DNA Polymerase High Fidelity (ThermoFisher, Carlsbad, CA), and 100−140 ng of genomic template DNA. The PCR temperature profile was as follows: (i) an initial melting step at 95 °C for 5 min, (ii) 25 cycles consisting of 95 °C for 40 s, 55 °C for 2 min and 72 °C for 1 min, and (iii) final elongation at 72 °C for 7 min. An index PCR and an amplicon clean-up were conducted subsequently according to Illumina-guidance (San Diego, CA, USA). The amplicons were pooled and sequenced on the Illumina MiSeq platform through MiSeq Reagent Kit V2 with paired-end 2 × 250 base reads by Protein and Nucleic Acid Facility (PAN, Stanford, CA). The raw sequences were deposited via the NCBI Sequence Read Archive (SRA) system under the accession numbers SRR10074424 − 10074435 for the pilot-scale reactor and SRX6720597 − SRX6720601 for SBR-2. The bacterial operational taxonomic units (OTUs) were identified using the Mothur platform (Kozich et al., 2013) with the SILVA reference file. 80,000 reads per sample were randomly selected from the raw sequences in the pilot-scale reactor samples, via the sub.sample command in Mothur and filtered generating more than 40,000 sequences for the ten samples, except day 194 and 235, which have about 2,000 and 9,000 sequences respectively. The relative composition of the microbial communities was established after removing members with abundance less than 1%.

Family-based Non-metric multidimensional scaling (NMDS) was conducted to visualize dynamics in microbial community structures over long-term operation of the pilot-scale reactor and the bench-scale SBR-2. NMDS was performed on 16S rRNA amplicon sequencing results at family level using Bray-Curtis distance ordination. Both the computed stress (<10) and instability ($<10^{-4}$) satisfied the corresponding criteria (McCune et al., 2002). NMDS analysis was conducted in R v. 3.6.1 programming environment using the package "vegan" v.2.5−6 (Oksanen et al., 2010).

2.5. RNA extraction and real-time PCR of nirS

Two sets of triplicates of 1 mL of mixed liquor samples was collected from the pilot-scale SBR at each different time point during an operational cycle. One set of samples were centrifuged immediately and resuspended in 1 mL of RNAlater (Thermo Fisher, MA, USA) solution before storing at −20 °C. The purification of miRNA and total RNA was carried out with miRNeasy Micro Kit (QIAGEN, MD, USA) per manufacturer's protocol after a 10x dilution of each sample. On-column DNase digestion was done using QIAGEN RNase-Free DNase kit. The RNA QC was done with Thermo Fisher NanoDrop OD reading and Agilent Bio-analyzer NanoChip. cDNA was synthesized with iScript cDNA Synthesis Kit (Bio-Rad, CA, USA). 10 ng of RNA template from each sample was used for the 20 μL of cDNA synthesis dissolved in the designated nuclease-free water. 1 μL of cDNA template was used for a reaction of quantitative-PCR (qPCR) to detect *nirS* gene using the primer set nirScd3aF/nirSR3cd (Throbäck et al., 2004; Kandeler et al., 2006; Wei et al., 2015). The other set of samples were used for extraction of genomic DNA following the method described in Section 2.4. qPCR calibration and measurement of the 16S rRNA gene was carried out using genomic DNA; qPCR of the *nirS* gene was carried out using cDNA (Scherson et al., 2013). To quantify *nirS* expression, the transcript abundance of *nirS* gene was normalized to the abundance of the 16S rRNA gene.

2.6. Nitrite removal, N_2O conversion, N_2O yield, PHA conversion and utilization

Three parameters were used to quantify the efficiencies of nitrite removal and N_2O production, and two parameters were used to quantify the synthesis and utilization of PHA as defined by the following equations:

$$NO_2^- \text{ removal efficiency} = \left(1 - \frac{[NO_2^-]_{Effluent} \times V_{Effluent}}{[NO_2^-]_{Influent} \times V_{Influent}}\right) \times 100\% \quad (1)$$

$$N_2O \text{ conversion efficiency} = \frac{[N_2O]_{aq} \times 2 \times V_{Total\ Liquid} + [N_2O]_{gas} \times 2 \times V_{Headspace}}{[NO_2^-]_{Influent} \times V_{Influent} - [NO_2^-]_{Effluent} \times V_{Total\ Liquid}} \times 100\% \quad (2)$$

$$N_2O \text{ yield} = \frac{[N_2O]_{aq} \times 2 \times V_{Total\ Liquid} + [N_2O]_{gas} \times 2 \times V_{Headspace}}{[NO_2^-]_{Influent} \times V_{Influent}} \times 100\% \quad (3)$$

$$PHA \text{ conversion yield} = \frac{[PHA]_{final\_anaerobic} - [PHA]_{initial\_anaerobic}}{[Acetate]_{initial\_anerobic} - [Acetate]_{final\_anaerobic}} \quad (4)$$

(expressed as gCOD-PHA/gCOD-Ac, or molC-PHA/molC-Ac; gCOD-PHA = [HB] × 144 gCOD/mol + [HV] × 192 gCOD/mol)

$$PHA \text{ utilization efficiency} = \frac{[PHA]_{initial\_anoxic} - [PHA]_{final\_anoxic}}{[NO_2^-]_{initial\_anoxic} - [NO_2^-]_{final\_anoxic}} \quad (5)$$

(expressed as gCOD-PHA/gN-NO_2^-)

Dissolved N_2O concentrations, $[N_2O]_{aq}$, were monitored using an in-situ probe in both the pilot and follow-up bench scale studies. In the pilot-scale reactor, N_2O in the gas phase was found to be present at levels less than equilibrium and gas mixing was insufficient, preventing use of measured $[N_2O]_{aq}$ for calculation of N_2O conversion efficiencies and yields. This issue was corrected in follow-up bench-scale studies using well mixed reactors and small headspace volumes that were only flushed during periods of stripping. Independent measurements of gas and liquid phase N_2O concentrations confirmed equilibrium conditions within both reactors. Accordingly, N_2O conversion efficiencies and yields, estimated using Henry's constant ($H_{N2O} = 2.4 \cdot 10^{-2}$ M bar^{-1}), are only reported for the bench-scale reactors.

3. Results and discussion

3.1. Long-term nitrous oxide production

Performance of the pilot-scale reactor and the bench-scale reactors was monitored and compared during long-term operation. In the pilot-scale SBR, MLVSS was stable at 2750 ± 410 mg/L and average dissolved N_2O at the end of the anoxic phase was 6 ± 3 mg N/L. Occasional overdose of polyamide-based coagulant resulted in the release of organic particulates from the upstream centrifuge, which passed through the nitritation reactor. As a result, coagulated organic particulates were transferred into the nitrous denitritation reactor together with nitrite at the end of each anaerobic phase, increasing the COD/N input ratio while simultaneously loading the reactor with organic carbon and nitrogen, preventing the desired decoupling of carbon and nitrogen inputs needed for PHA and N_2O production (Scherson et al., 2013, 2014; Gao et al., 2017). A settling tank was then added to remove the coagulated solids in the nitrified centrate. Production of N_2O was unstable, and an upstream nitrate perturbation (days 250–260) likely also contributed to the low N_2O yields. After switching to a surrogate nitrified centrate feed on day 258 and decreasing the anaerobic period to 7 h, N_2O production increased dramatically (Fig. S4 and Table S1). On day 305, nitrogen loading was doubled to 2.0 kg N/m^3-d and aqueous N_2O concentration further increased to 35 mg N/L.

Because of time constraints on the pilot study, follow up bench-scale studies were performed. These studies focused on the impacts of the relative lengths of the anaerobic and anoxic periods. The two SBRs were inoculated with the pilot-scale reactor biomass and operated with similar start-up conditions but with different anaerobic phase durations. After 30 days of operation, both reactors reached MLVSS levels exceeding 3,000 mg/L, and performance of the two reactors differed dramatically.

During operation with a 12-h anaerobic phase, SBR-1 was similar to the pilot reactor, with transient production of N_2O (Fig. 2a). The average nitrite removal efficiency was 94% (±12%, n = 150) from day 100–250. Wildly fluctuating N_2O production was observed, with average yield below 30%. Residual nitrite was partly decanted and discharged after settling, and partly carried over to the next cycle in SBR-1. To ensure sufficient reducing equivalents were available for nitrite reduction to N_2O, acetate input was increased while keeping nitrite input constant on day 300, resulting in a COD/N input ratio increase from 3.0 to 3.5. Improved nitrite removal efficiency (96% ± 2%, n = 150) was observed from day 300 to day 450 with statistical significance (Student's t-test, $p = 1.25 \times 10^{-8}$). After a further increase in COD/N ratio, N_2O production resumed on day 370 but the N_2O yield continued to fluctuate.

SBR-2 was operated for 600 days and achieved stable N_2O production during operation with an 8-h anaerobic phase (Fig. 2b). After 90 days of startup, MLVSS levels reached 3000 mg/L. N_2O production was unstable during startup, but the rate of nitrogen removal rate was stable at 95%. N_2O production stabilized after 150 days of operation. From day 150–300, the average nitrogen removal rate was 96% (±6%, n = 150), with an N_2O yield of 70% (±16%, n = 45). Similarly, the input ratio of COD/N was increased from 3.0 to 3.5 from day 300 onwards to ensure sufficient electron donor for nitrite removal. As a result, the average nitrogen removal rate increased to 98% (±3%, n = 150) from day 350–500, a statistically significant improvement over days 150–300 (Student's t-test, $p = 1.25 \times 10^{-8}$). In addition, this change in SBR-2 supported greater biomass accumulation: a near doubling of MLVSS occurred, with measured values approaching 6,000 mg/L (Fig. S8, Table 1). The elevated biomass levels that resulted from increased COD/N input ratios led to an increase in anaerobic acetate uptake from 45 mgCOD/L-h to 114 mgCOD/L-h, whereas the specific acetate uptake rates remained constant (from 0.015 to 0.018 mgCOD-Ac/mgCOD-VSS-h). This enabled further shortening of the anaerobic phase to 7 h and shortening of the anoxic phase to 4 h, decreasing total cycle time to 12 h and enabling an increase in N_2O yield to 87% on days 535–600.

Table 1 compares key operational parameters for the three SBRs. In all cases, a decrease in anaerobic phase duration resulted in more efficient and stable N_2O production. After switching to a 12-h cycle with a 4-h anaerobic phase, SBR-2 achieved high volumetric nitrogen loading rates (0.25 kg N/m^3-d) with efficient N_2O production. Decreasing the cycle time from 24 h to 12 h resulted in a 50% decrease in HRT (i.e., from 4 days to 2 days).

3.2. PHA utilization and denitritation

Polyhydroxyalkanoate (PHA) granules provide the reducing power needed to drive reduction of nitrite to N_2O (Scherson et al.,

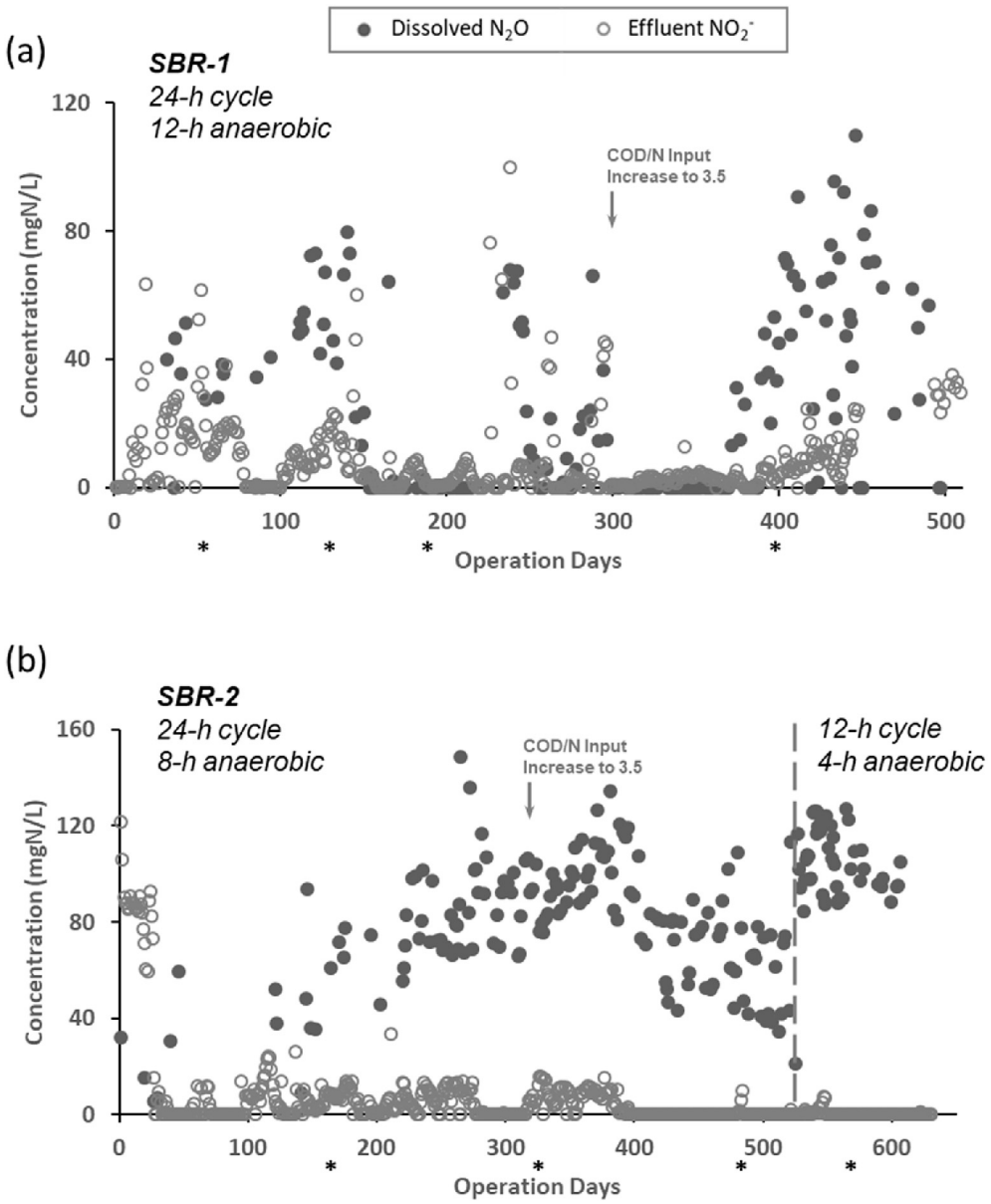

Fig. 2. Dissolved N_2O concentrations at the end of the anoxic periods: (a) bench-scale SBR-1 (12-h anaerobic period; 24-h cycle time), and (b) bench-scale SBR-2 (8-h anaerobic period; 24-h and 12-h cycle times). Intensively sampled cycles are marked with an asterisk symbol (*).

Table 1
Summary of operational parameters for pilot-scale and lab-scale nitrous denitritation reactors.

	Pilot-scale SBR		Follow-up Bench-scale 1	Follow-up Bench-scale 2	
Anaerobic Phase, t_{An} (h)	12	7	12	8	**4**
Total Cycle Time, t_C (h)	24	24	24	24	**12**
Hydraulic Residence Time, HRT (d)	10	10	4	4	**2**
Solid Retention Time, SRT (d)	60	60	60	60	**30**
Mixed Liquor Suspended Solid, MLTSS/MLVSS (mg/L)	2600 ± 607/2444 ± 537	3025 ± 86/2809 ± 86	2569 ± 397/2326 ± 402	3354 ± 375/3134 ± 361	**6389 ± 457/6098 ± 484**
Performance Stability	-	-	-	+	++
Maximum Nitrogen Loading (kgN/m^3/d)	0.1	0.2	0.12	0.12	**0.25**
No. of Operational Cycles	126	26	497	301	**170**

2014). Accumulation of PHA depends upon the relative rates of PHA polymerization and depolymerization (Arias et al., 2013). Fig. 3 illustrates changes in PHA levels for two intensively sampled operational cycles in the pilot reactor. For a 11-h anaerobic phase and a total cycle time of 24 h (Fig. 3a), PHA levels increased for the first 8 h then declined for hours 8–11, likely due to decay. During

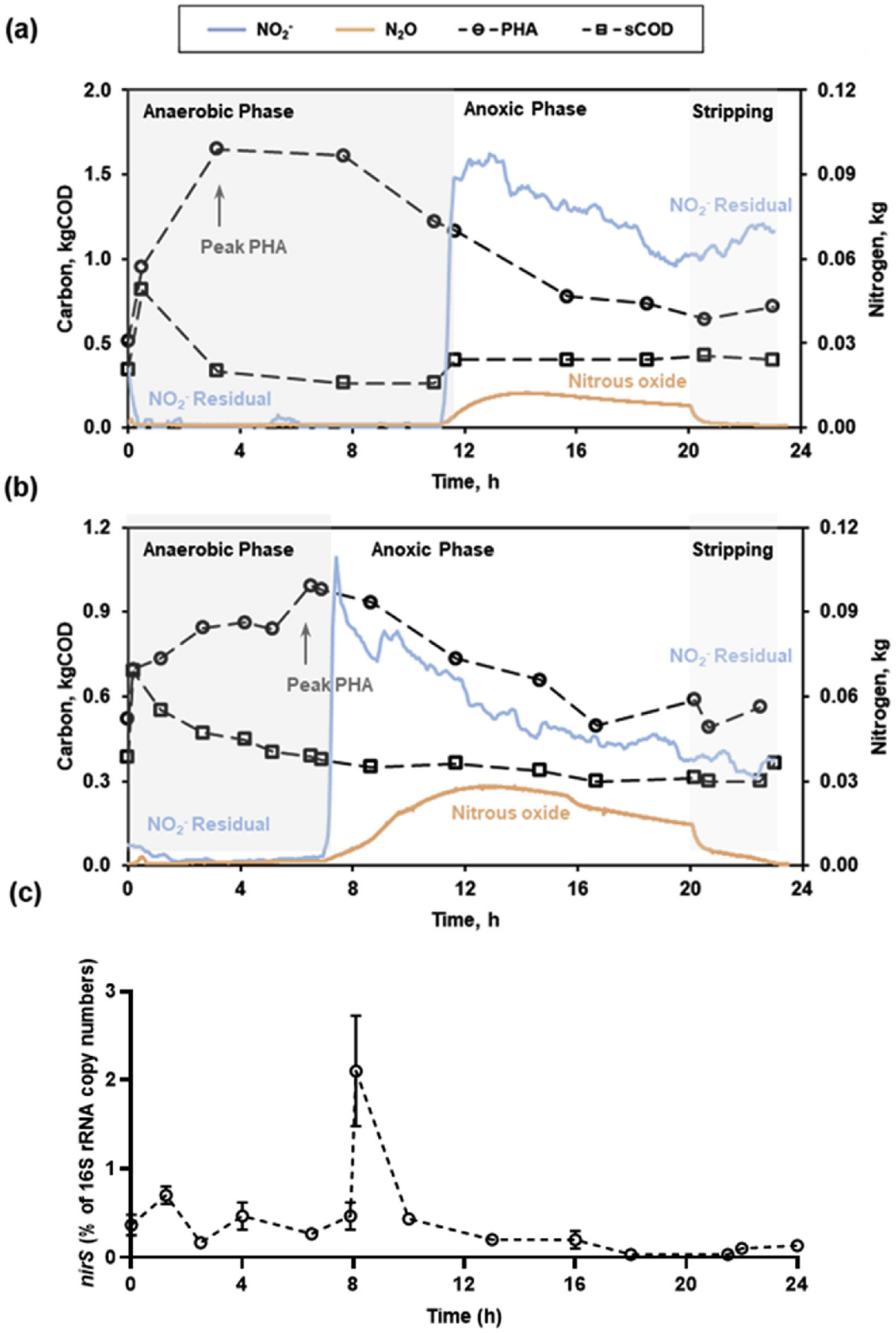

Fig. 3. Performance of the pilot-scale SBR during (a) period I with a 12-h anaerobic phase (day 265) and (b) period II with a 7-h anaerobic phase (day 309). (c) The transcript abundance of *nirS* normalized by 16S rRNA gene abundance during a 24-h cycle (day 309). Open circles show PHA content (PHB only): blue and orange lines are continuous probe recordings of nitrite and N_2O concentrations, respectively, in the aqueous phase. (For interpretation of the references to color in this figure legend, the reader is referred to the Web version of this article.)

the subsequent 13-h anoxic phase, PHA levels continued to decrease due to decay and also due to oxidation of PHB by nitrite with coupled reduction of nitrite to N2O. Residual nitrite was partly wasted and partly carried over to the anaerobic phase of the subsequent cycle, where the added acetate drove complete denitrification to N_2 rather than N_2O. The observed PHA utilization

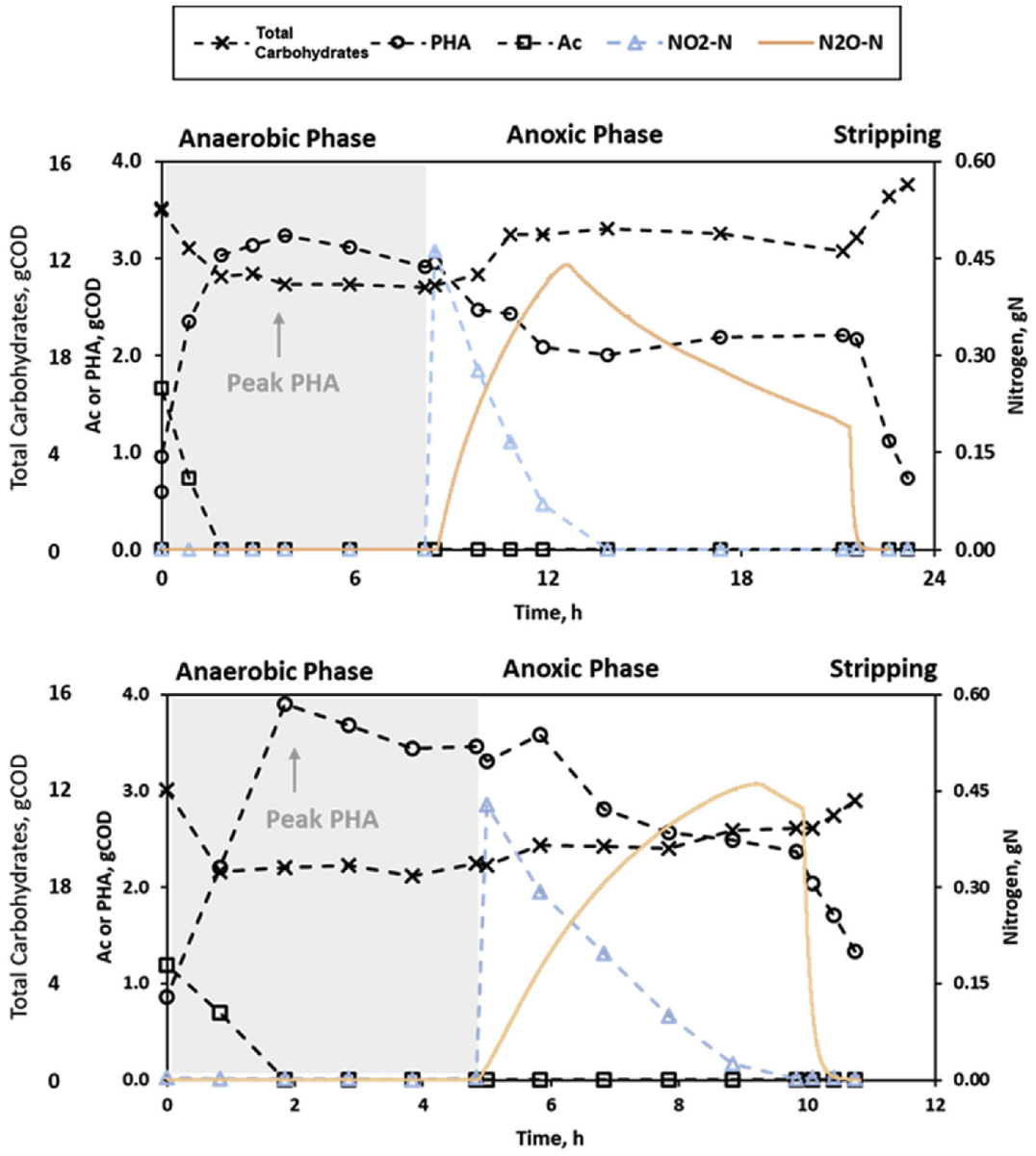

Fig. 4. A comparison of (a) a 24-h (day 507) and (b) a 12-h (day 520) operation cycle for bench-scale SBR-2 before and after optimization. Dissolved N_2O concentrations were continuously recorded by microsensor. All other concentrations were analytical measurements from samples taken at discrete time points. Changes in total carbohydrates reflects changes in intracellular glycogen.

efficiency was 20 gCOD/gN ratio, a very large value reflecting inefficient use of PHA for N2O production. Over many cycles, however, production and consumption of N_2O was observed, suggesting that shortening of the anoxic period could limit PHA consumption and improve recovery of N_2O (Fig. S2). Accordingly, the anaerobic phase was decreased to 7 h, and a PHA utilization efficiency of 3.9 gCOD-PHA/gN-NO2- was obtained (Fig. 3b), as dissolved N_2O levels increased to 13 mg N/L. The conversion yield of acetate to PHA in COD units improved to 70%. To maintain a constant cycle time, the anoxic phase was extended to 13.5 h. Under these conditions, nitrite removal efficiency increased to 96%, but residual nitrite persisted and was carried over to the next operational cycle.

The impacts of a shortened anaerobic period and a shortened anoxic period were further evaluated and compared over an extended period of operation in bench-scale reactors SBR-1 and SBR-2. Both reactors were initially operated at the same HRT and cycle time, but SBR-1 was subject to a longer anaerobic phase (12 h) than SBR-2 (8 h, then 4 h). The extended anaerobic period evaluated in SBR-1 selected for unstable operational performance whereas the shortened anaerobic period evaluated in SBR-2 selected for both a stable community and stable long-term performance.

In SBR-1, three distinct patterns of nitrite consumption were observed (Fig. S3) as the microbial community changed: in the first (Fig. S3a), nitrite residual from the anoxic phase carried over into the anaerobic phase of the next cycle (as in the pilot reactor); in the second (Fig. S3b), nitrite was reduced sequentially to N_2O then N_2 in the anoxic phase and these steps were coupled to PHA accumulation, PHA consumption, and cell growth; in the third (Fig. S3c), nitrite residual was eliminated, with complete acetate assimilation during the anaerobic phase (similar to SBR-2, described below). The negative impact of residual nitrite led to unstable N_2O production during long-term operation of SBR-1 (Fig. 2a).

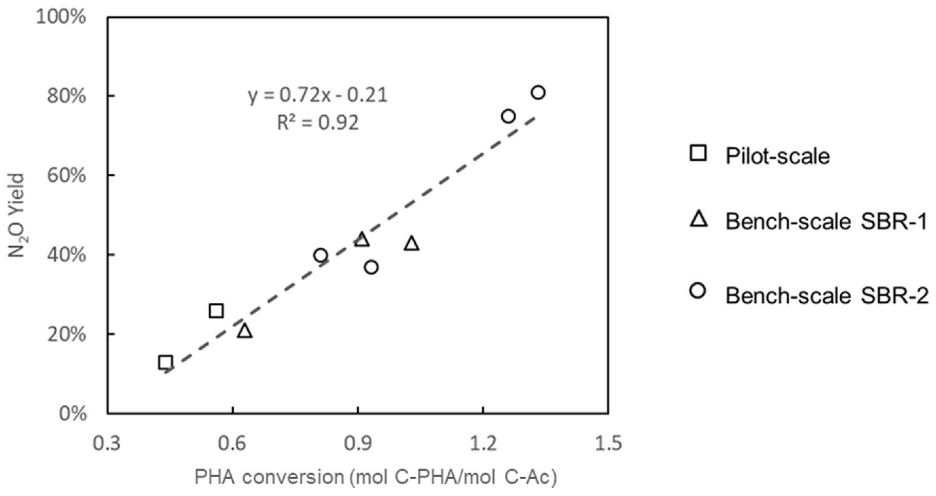

Fig. 5. Linear correlation between nitrous oxide production yield and PHA conversion yield (mole C/mole C). Each data point on represents one intensively sampled operational cycle in pilot-scale SBR (squares), bench-scale SBR-1 (triangles) or SBR-2 (circles). The N_2O yields in the pilot-scale SBR were estimated based on dissolved N_2O concentrations.

In SBR-2, a stable pattern similar to the third pattern of SBR-1 emerged after ~200 days of operation (Fig. S3d): acetate was incorporated into PHA during the anaerobic phase, with efficient and stable N_2O production in the anoxic phase. Acetate uptake and PHA synthesis was driven by oxidation of glycogen (Fig. 4). A similar study implicated denitrifying glycogen-accumulating organisms as likely N_2O producers (Zeng et al., 2003). The conversion yield of acetate to PHA was 93% during the anaerobic phase. When nitrite was added at peak PHA levels, nitrite removal efficiency was 94%, and N_2O yield reached 74% (Fig. S3d). Efficient utilization of PHA was achieved, as the consumption ratio of PHA to nitrite reached 2.4 gCOD/gN. N_2O was stripped by air and recovered at peak concentration. After increasing the COD/N input ratio, rapid PHA accumulation was accompanied by increased biomass concentrations, suggesting the feasibility of a shortened anaerobic phase. Simultaneously, though, the elongated anoxic phase that resulted after nitrite depletion resulted in further reduction of N_2O to N_2, decreasing N_2O yield before stripping. Accordingly, on day 520, the duration of the anaerobic and the anoxic phases were reduced to 5 h apiece in a 12-h cycle (Fig. 4b). N_2O yield increased from 43% to 87%, and the volumetric loading rate of nitrogen doubled, reaching 0.25 kg N/m^3-d. Decreasing the operational cycle in SBR-2 to from 24 h to 12 h minimized PHA fermentation during the anoxic phase, and improved PHA utilization efficiency to 2.4 gCOD-PHA/gN-NO2- (Fig. 4). The bench-scale testing thus successfully addressed the concern of PHA insufficiency encountered during pilot-scale testing.

Comparing PHA synthesis and utilization for nitrous denitritation from all three systems studied, a positive linear correlation was observed between PHA synthesized per acetate (mol C/mol C) at the end of anaerobic phase and N_2O yield during anoxic phase (ANOVA, $F(1,7) = 84.78$, $p < 0.001$), with an R^2 of 0.92 (Fig. 5). Minimizing PHA fermentation improves the PHA/Ac ratio. A gradual increase in N_2O production accompanied improved efficiency of carbon storage was shown from pilot-scale to bench-scale SBR-1 and SBR-2. The linear relationship predicts that as the PHA/Ac ratio approaches 1.7, N_2O production from nitrite approaches 100%. A similar linear correlation between efficiency of carbon storage as PHA and N_2O accumulation for mixed heterotrophic denitrifying cultures has been previously reported (Liu et al., 2015). Notably, the PHA/Ac ratio exceeded one in SBR-2 as the monitored PHA included both HB and HV monomers. The HV monomers derive from glycogen, as expected based upon the known biochemical pathways of GAOs. A proposed model and experimental observations reported PHA/Ac ratios ranging from 1.65 to 1.91 for GAOs (Filipe et al., 2001; Zeng et al., 2002). This ratio may thus be a good indicator of the relative abundance of denitrifying GAOs, the efficiency of carbon utilization, and capacity for N_2O production across systems with different microbial community structures.

3.3. Mechanisms of N_2O production and consumption

The timing of nitrite addition had a significant impact on N_2O production. As shown in Fig. 3, shortening the anaerobic phase to coincide with peak PHA significantly improved N_2O production. The expression of *nirS* was observed immediately after nitrite addition (Fig. 3c), which exhibited an immediate tenfold increase in transcript abundance. When acetate levels decreased to zero, reduction of nitrite to N_2O was coupled to PHA oxidation. Further reduction of N_2O to N_2 may have been limited by competition for reducing equivalents, or nitrous oxide reductase may have been inhibited due to high levels of inhibitory free nitrous acid (FNA) (Richardson et al., 2009). As nitrite was consumed and FNA levels fell from 2 to 0.8 μg N/L (Anthonisen et al., 1976), inhibition of nitrous oxide reduction may have been alleviated enabling production of N_2 (Zhou et al., 2008). Similar observations of cascading denitrification reactions, inhibitory intermediates, and competition for electrons have been reported, especially under electron donor-limited conditions (Pan et al., 2013; Wang et al., 2018).

Diverse microbial communities were selected by the operating conditions of the nitrous denitritation reactors. In the pilot-scale reactor, bacteria from the families *Comamonadaceae*, *Xanthomonadaceae*, and *Zoogloeaceae* were enriched and identified by 16S amplicon sequencing. A stable community structure established by day 194, coinciding with a stable pattern of N_2O production. The dominant genus was a *Diaphorobacter* strain (Woo, 2017). *D. nitroreducens* and *D. polyhydroxybutyrativorans* both have the genes required for denitrification and for PHA synthesis and degradation (Tabrez Khan and Hiraishi, 2002; Zuo et al., 2015). Perturbations in the microbial communities correlated with upsets in upstream nitritation and operational changes (Fig. 6a). A

Fig. 6. Amplicon sequencing results for bacterial 16S rRNA genes in (a) the pilot nitrous denitritation SBR and (b) bench-scale SBR-2 over long-term operation. For details of the color scheme in the legend, please refer to Supplementary Data Fig. S6. (For interpretation of the references to color in this figure legend, the reader is referred to the Web version of this article.)

significant change in the relative abundance of *Paracoccus* occurred on day 257, likely due to an increase in nitrate in the feed. *Paracoccus denitrificans* is a facultative denitrifier possessing both nitrate and nitrite reductase, and respiratory nitrate reductase (NAP) is preferentially expressed under carbon or nutrient limiting conditions (Blaszczyk, 1993; Sears et al., 1997). *Paracoccus* also possesses genes for both PHA synthase and depolymerase (Gao et al., 2001). *Thauera* species are heterotrophic denitrifiers (Philipp and Schink, 2012) that can accumulate PHA in full-scale wastewater treatment plants (Oshiki et al., 2008). They became more prevalent when the influent was switched to surrogate nitrified centrate and persisted when the influent was switched back to effluent from the nitritation reactor.

Among the identified N_2O producing candidates, *Diaphorobacter* possesses *nirK* genes encoding for nitrite reductase, whereas *Thauera* and *Comamonas* possess *nirS* genes (Heylen et al., 2006). *Paracoccus* has both *nirS* and *nirK* genes. Therefore, *nirS* primers were able to track the expression of nitrite reductase encoding genes in the pilot-scale denitritation SBR, when its microbial community contained mainly *Thauera* and *Paracoccus*. The *nirS* primer, nirScd3aF/nirSR3cd, used in this study, has been widely used for pure cultures including *Paracoccus* as well as for environmental samples (Throbäck et al., 2004; Kandeler et al., 2006; Wei et al., 2015). The expression of *nirK* genes, on the other hand, showed no significant change over time. Moreover, *Thauera*, *Comamonas* and *Paracoccus* species were known to have genes encoding for nitrous oxide reductase (Hoeren et al., 1993; Liu et al., 2013; Throbäck et al., 2004). They might contribute to reduction of N_2O to nitrogen gas during an extended anoxic phase.

SBR-1 was inoculated with a seed from the pilot-scale reactor. Over its 500 days of operation, the bacterial community experienced significant shifts in composition. *Thauera* that was likely transferred from the pilot-scale SBR dominated SBR-1 on day 351 constituting 43% of the 16S rDNA clones (Fig. S5a). Other potential N_2O-producing microorganisms, including *Diaphorobacter* and *Paracocus*, were detected. While both SBR-1 and SBR-2 were seeded by the pilot reactor, the operational mode in SBR-2 selected against persistence of *Thauera* (Fig. 6b) and selected in favor of an uncultured *Defluviicoccus*-related strain, which comprised a majority of the 16S rDNA clones detected (Fig. S5b). The relative abundance of

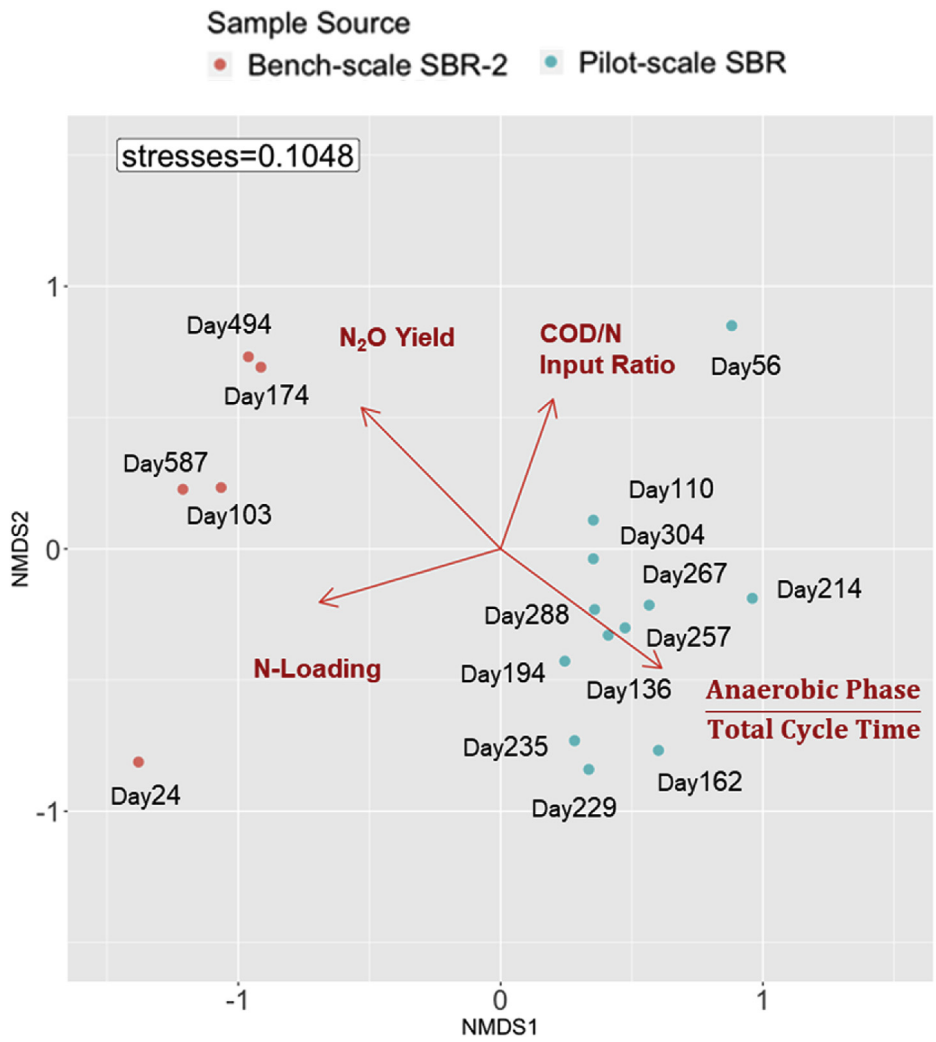

Fig. 7. NMDS plot of combined 16S rRNA amplicon sequencing results from the pilot-scale SBR and bench-scale reactor SBR-2. Each data point represents a sample taken on the noted operational day.

the *Defluviicoccus*-related strain (*Rhodospirillaceae* family) was stable at 37–39% for days 494–587. Full-length 16S rRNA clone library results for dominant denitrifying glycogen accumulating organisms (GAOs) in the SBR showed only 92% similarity to *Defluviicoccus vanus* (cluster I, Fig. S7). The closest match with a 99% similarity is to a sequence from an uncultured *Defluviicoccus* clone recently designated as the sole member of cluster IV (McIlroy et al., 2009). To date, none of the *Defluviicoccus*-related GAOs have genes for complete denitrification. Cluster I *Defluviicoccus*-related GAOs were reportedly able to reduce nitrate, but not nitrite (Wang et al., 2008). According to a recent metagenomic study (Wang et al., 2014), Cluster II *Defluviicoccus*-related GAOs reportedly lack dissimilatory denitrification genes. Addition of nitrite for enhanced biological phosphorus removal (EBPR) is postulated to suppress growth of GAOs (Tayà et al., 2013). In this study, however, *Defluviicoccus* Cluster IV were enriched and became dominant, and the reactor produced N_2O under stable operating conditions. It thus appears likely that these organisms are responsible for carbon storage and for nitrous denitritation, but additional studies are needed to confirm such phenotype within Cluster IV *Defluviicoccus*. GAOs have been previously implicated in the production of N_2O (Zeng et al., 2003). Relatively shorter anaerobic phase in SBR-2 enriched for bacteria with more rapid acetate uptake, where GAO exhibited competitive advantages with glycogen-driven acetate uptake and PHA synthesis.

As shown in the NMDS plot of Fig. 7, two distinct clusters reveal that the microbial communities of the pilot-scale reactor differed significantly from those of bench-scale SBR-2 on a two-dimensional ordination (stress = 0.10, r^2 = 0.94). As expected, the inoculum of the pilot-scale bioreactor and that of SBR-2 clustered at different locations. Shifts in community structure of the bench-scale reactor after transferring an inoculum from the pilot-scale reactor are also evident. Overlaying the key operational parameters as vectors, an increase in the duration of anaerobic phase correlated negatively with N_2O yields (Table S3). Moreover, the microbial communities in the pilot-scale SBR (day288–304) and bench-scale SBR-2 (day103–587) shifted towards clusters with a higher N_2O yield, likely due to the shortened anaerobic phase and increased nitrogen loading (Fig. 7). Other factors not assessed in this study could be associated with the observed shifts in community structure.

3.4. Application of CANDO in sidestream nitrogen removal

The highest volumetric nitrogen loading rate achieved to date for CANDO is 0.25 kg N/m^3-d - the maximum loading rate attained for SBR-2 in this study. This value is comparable to other sidestream

treatment processes, such as Anammox, but needs validation at pilot scale. The benefits of CANDO as a shortcut nitrogen removal process include a reduced aeration requirement, savings in reducing equivalents, reduction in biosolid production, and potential for energy recovery (Gao et al., 2014). A recent stoichiometry study has verified the low biomass yield that results from alternating consumption and storage of organic carbon in CANDO (Wang et al., 2020).

Additional CANDO pilot-scale testing is needed, now with the benefit of hindsight provided by this study. We note that many of the unexpected operational issues that resulted in operational upsets originated in the upstream pilot-scale nitritation reactor (e.g., polymer addition, centrifuge performance, pH control, DO control). This calls for more attention to upstream process control in general. Performance of the nitritation stage is also an issue common to other shortcut nitrogen removal processes. A significant operational cost is the cost of carbon source (e.g., sodium acetate, acetic acid) for pilot-scale testing. Such costs can potentially be reduced by using primary effluent in full-scale applications (Weißbach et al., 2018b). Such a system needs evaluation at pilot scale. A final challenge is low-energy recovery of dissolved N_2O, for example, by application of membrane-based stripping (Weißbach et al., 2018a). This too requires evaluation at pilot scale.

4. Conclusions

A key insight from this work is the finding that the relative duration of anaerobic and anoxic phases is crucial to efficient N_2O production. Especially important is management of PHA, a key electron storage compound. Scheduling of nitrite addition to coincide with peak PHA accumulation ensures efficient use of reducing equivalents for nitrite reduction to N_2O. Long-term operation of bench-scale reactors with different anaerobic/anoxic schedules enriched for distinctive microorganisms with different patterns of PHA accumulation and denitritation. Shortening of the anaerobic and anoxic phases improved yield and enabled stable production of N_2O at both pilot- and bench-scale.

Declaration of competing interest

The authors declare that they have no known competing financial interests or personal relationships that could have appeared to influence the work reported in this paper.

Acknowledgement

This research was supported by the U.S. National Science Foundation Engineering Research Center Reinventing the Nation's Urban Water Infrastructure (ReNUWIt) [grant number EEC-1028968], and by the National Cheng Kung University North America Alumni Association and Foundation. The initial construction of the pilot-scale reactor was supported by an Innovation Transfer Grant from TomKat Center for Sustainable Energy. We are extremely grateful to Delta Diablo for financial and operational support of the pilot-scale system as a partner on EPA Grant [EPA-R9-WTR3-13-001, grant number 99T07401]. We thank Gary Darling, Amanda Roa, Nick Steiner and Operations, Lab and Maintenance staff.

Appendix A. Supplementary data

Supplementary data to this article can be found online at https://doi.org/10.1016/j.watres.2020.115575.

References

Liu, B., Mao, Y., Bergaust, L., Bakken, L.R., Frostegård, Å., 2013. Strains in the genus *Thauera* exhibit remarkably different denitrification regulatory phenotypes. Environ. Times. https://doi.org/10.1111/1462-2920.12142. Microbiol. 15, n/a-n/a.

Anthonisen, A.C., Loehr, R.C., Prakasam, T.B., Srinath, E.G., 1976. Inhibition of nitrification by ammonia and nitrous acid. J. Water Pollut. Control Fed. 48, 835–852.

Arias, S., Bassas-Galia, M., Molinari, G., Timmis, K.N., 2013. Tight coupling of polymerization and depolymerization of polyhydroxyalkanoates ensures efficient management of carbon resources in *Pseudomonas putida*. Microb. Biotechnol. 6, 551–563. https://doi.org/10.1111/1751-7915.12040.

Blaszczyk, M., 1993. Effect of medium composition on the denitrification of nitrate by *Paracoccus denitrificans*. Appl. Environ. Microbiol. 59, 3951–3953.

East Bay Municipal Utility District (EBMUD) and Project Partners, 2017. Reducing Nutrients in the San Francisco Bay through Additional Wastewater Treatment Plant Sidestream Treatment. Final Report for EPA Sidestream Nutrient Removal Study, Oakland, CA.

Filipe, C.D., Daigger, G.T., Grady, C.P., 2001. Stoichiometry and kinetics of acetate uptake under anaerobic conditions by an enriched culture of phosphorus-accumulating organisms at different pHs. Biotechnol. Bioeng. 76, 32–43. https://doi.org/10.1002/bit.1022.

Fowler, D., Coyle, M., Skiba, U., Sutton, M.A., Cape, J.N., Reis, S., Sheppard, L.J., Jenkins, A., Grizzetti, B., Galloway, J.N., Vitousek, P., Leach, A., Bouwman, A.F., Butterbach-Bahl, K., Dentener, F., Stevenson, D., Amann, M., Voss, M., 2013. The global nitrogen cycle in the twenty-first century. Philos. Trans. R. Soc. B Biol. Sci. 368 https://doi.org/10.1098/rstb.2013.0164, 20130164–20130164.

Gao, D., Maehara, A., Yamane, T., Ueda, S., 2001. Identification of the intracellular polyhydroxyalkanoate depolymerase gene of *Paracoccus denitrificans* and some properties of the gene product. FEMS Microbiol. Lett. 196, 159–164. https://doi.org/10.1016/S0378-1097(01)00061-1.

Gao, H., Scherson, Y.D., Wells, G.F., 2014. Towards energy neutral wastewater treatment: methodology and state of the art. Environ. Sci. Process. Impacts 16, 1223–1246. https://doi.org/10.1039/c4em00069b.

Gao, H., Liu, M., Griffin, J.S., Xu, L., Xiang, D., Scherson, Y.D., Liu, W.-T., Wells, G.F., 2017. Complete nutrient removal coupled to nitrous oxide production as a bioenergy source by denitrifying polyphosphate-accumulating organisms. Environ. Sci. Technol. 51, 4531–4540. https://doi.org/10.1021/acs.est.6b04896.

Gerhardt, P., Wood, W.A., Krieg, N.R., Murray, R., 1994. Methods for General and Molecular Bacteriology. American Society for Microbiology. https://doi.org/10.1002/food.19960400226.

Hellinga, C., Schellen, A., Mulder, J., van Loosdrecht, M.C.M., Heijnen, J., 1998. The SHARON process: an innovative method for nitrogen removal from ammonium rich waste water. Water Wastewater Syst 37, 135–142. https://doi.org/10.1016/S0273-1223(98)00281-9.

Heylen, K., Gevers, D., Vanparys, B., Wittebolle, L., Geets, J., Boon, N., Vos, P. De, De Vos, P., 2006. The incidence of *nirS* and *nirK* and their genetic heterogeneity in cultivated denitrifiers. Environ. Microbiol. 8, 2012–2021. https://doi.org/10.1111/j.1462-2920.2006.01081.x.

Hoeren, F.U., Berks, B.C., Ferguson, S.J., McCarthy, J.E., 1993. Sequence and expression of the gene encoding the respiratory nitrous-oxide reductase from *Paracoccus denitrificans*. New and conserved structural and regulatory motifs. Eur. J. Biochem. 218, 49–57. https://doi.org/10.1111/j.1432-1033.1993.tb18350.x.

Kandeler, E., Deiglmayr, K., Tscherko, D., Bru, D., Philippot, L., 2006. Abundance of *narG, nirS, nirK*, and *nosZ* genes of denitrifying bacteria during primary successions of a glacier foreland. Appl. Environ. Microbiol. 72, 5957–5962. https://doi.org/10.1128/AEM.00439-06.

Klindworth, A., Pruesse, E., Schweer, T., Peplies, J., Quast, C., Horn, M., Glöckner, F.O., 2013. Evaluation of general 16S ribosomal RNA gene PCR primers for classical and next-generation sequencing-based diversity studies. Nucleic Acids Res. 41, 1–11. https://doi.org/10.1093/nar/gks808.

Kozich, J.J., Westcott, S.L., Baxter, N.T., Highlander, S.K., Schloss, P.D., 2013. Development of a dual-Index sequencing strategy and curation pipeline for analyzing amplicon sequence data on the MiSeq Illumina sequencing platform. Appl. Environ. Microbiol. 79, 5112–5120. https://doi.org/10.1128/AEM.01043-13.

Lackner, S., Gilbert, E.M., Vlaeminck, S.E., Joss, A., Horn, H., van Loosdrecht, M.C.M., 2014. Full-scale partial nitritation/anammox experiences – an application survey. Water Res. 55, 292–303. https://doi.org/10.1016/j.watres.2014.02.032.

Liu, Y., Peng, L., Guo, J., Chen, X., Yuan, Z., Ni, B.-J., 2015. Evaluating the role of microbial internal storage turnover on nitrous oxide accumulation during denitrification. Sci. Rep. 5, 15138. https://doi.org/10.1038/srep15138.

Massara, T.M., Malamis, S., Guisasola, A., Baeza, J.A., Noutsopoulos, C., Katsou, E., 2017. A review on nitrous oxide (N_2O) emissions during biological nutrient removal from municipal wastewater and sludge reject water. Sci. Total Environ. 596–597, 106–123. https://doi.org/10.1016/j.scitotenv.2017.03.191.

McCune, B., Grace, James, 2002. Analysis of Ecological Communities. MJM Software Design, Gleneden Beach, OR.

McIlroy, S., Seviour, R.J., 2009. Elucidating further phylogenetic diversity among the *Defluviicoccus*-related glycogen-accumulating organisms in activated sludge. Environ. Microbiol. Rep. 1, 563–568. https://doi.org/10.1111/j.1758-2229.2009.00082.x.

Myung, J., Wang, Z., Yuan, T., Zhang, P., Van Nostrand, J.D., Zhou, J., Criddle, C.S., 2015. Production of nitrous oxide from nitrite in stable type II methanotrophic enrichments. Environ. Sci. Technol. 49 (18), 10969–10975. https://doi.org/10.1021/acs.est.5b03385.

Oksanen, J., Kindt, R., Legendre, P., Hara, B.O., Simpson, G.L., Solymos, P., Stevens, M.H.H., Wagner, H., 2010. Vegan: Community Ecology Package. R Package Version 1, 17-3. October.

Oshiki, M., Onuki, M., Satoh, H., Mino, T., 2008. PHA-accumulating microorganisms in full-scale wastewater treatment plants. Water Sci. Technol. https://doi.org/10.2166/wst.2008.652.

Pan, Y., Ni, B.J., Bond, P.L., Ye, L., Yuan, Z., 2013. Electron competition among nitrogen oxides reduction during methanol-utilizing denitrification in wastewater treatment. Water Res. 47, 3273–3281. https://doi.org/10.1016/j.watres.2013.02.054.

Philipp, B., Schink, B., 2012. Different strategies in anaerobic biodegradation of aromatic compounds: nitrate reducers versus strict anaerobes. Environ. Microbiol. Rep. 4, 469–478. https://doi.org/10.1111/j.1758-2229.2011.00304.x.

Rice, E.W., Baird, R.B., Eaton, A.D. (Eds.), 2017. Standard Methods for Examination of Water and Wastewater, 23rd ed. American Public Health Association, American Water Works Association, Water Environment Federation.

Richardson, D., Felgate, H., Watmough, N., Thomson, A., Baggs, E., 2009. Mitigating release of the potent greenhouse gas N_2O from the nitrogen cycle – could enzymic regulation hold the key? Trends Biotechnol. 27, 388–397. https://doi.org/10.1016/j.tibtech.2009.03.009.

Scherson, Y.D., Wells, G.F., Woo, S.-G., Lee, J., Park, J., Cantwell, B.J., Criddle, C.S., 2013. Nitrogen removal with energy recovery through N_2O decomposition. Energy Environ. Sci. 6, 241–248. https://doi.org/10.1039/C2EE22487A.

Scherson, Y.D., Woo, S.-G., Criddle, C.S., 2014. Production of nitrous oxide from anaerobic digester centrate and its use as a co-oxidant of biogas to enhance energy recovery. Environ. Sci. Technol. 48, 5612–5619. https://doi.org/10.1021/es501009j.

Sears, H.J., Spiro, S., Richardson, D.J., 1997. Effect of carbon substrate and aeration on nitrate reduction and expression of the periplasmic and membrane-bound nitrate reductases in carbon-limited continuous cultures of *Paracoccus denitrificans* Pd1222. Microbiology 143, 3767–3774. https://doi.org/10.1099/00221287-143-12-3767.

Selman, M., Greenhalgh, S., Diaz, R., Sugg, Z., 2008. Eutrophication and hypoxia in coastal areas: a global assessment of the state of knowledge why is eutrophication a problem? WRI Policy Note 1, 1–6.

Tabrez Khan, S., Hiraishi, A., 2002. Diaphorobacter nitroreducens gen. nov., sp. nov., a poly(3-hydroxybutyrate)-degrading denitrifying bacterium isolated from activated sludge. J. Gen. Appl. Microbiol. 48, 299–308. https://doi.org/10.2323/jgam.48.299.

Tayà, C., Garlapati, V.K., Guisasola, A., Baeza, J.A., 2013. The selective role of nitrite in the PAO/GAO competition. Chemosphere 93, 612–618. https://doi.org/10.1016/j.chemosphere.2013.06.006.

Throbäck, I.N., Enwall, K., Jarvis, A., Hallin, S., 2004. Reassessing PCR primers targeting *nirS*, *nirK* and *nosZ* genes for community surveys of denitrifying bacteria with DGGE. FEMS Microbiol. Ecol. 49, 401–417. https://doi.org/10.1016/j.femsec.2004.04.011.

Wang, X., Zeng, R.J., Dai, Y., Peng, Y., Yuan, Z., 2008. The denitrification capability of cluster 1 *Defluviicoccus vanus*-related glycogen-accumulating organisms. Biotechnol. Bioeng. 99, 1329–1336. https://doi.org/10.1002/bit.21711.

Wang, Z., Guo, F., Mao, Y., Xia, Y., Zhang, T., 2014. Metabolic characteristics of a glycogen-accumulating organism in Defluviicoccus Cluster II revealed by comparative genomics. Microb. Ecol. 68, 716–728. https://doi.org/10.1007/s00248-014-0440-3.

Wang, Y., Li, P., Zuo, J., Gong, Y., Wang, S., Shi, X., Zhang, M., 2018. Inhibition by free nitrous acid (FNA) and the electron competition of nitrite in nitrous oxide (N_2O) reduction during hydrogenotrophic denitrification. Chemosphere 213, 1–10. https://doi.org/10.1016/j.chemosphere.2018.08.135.

Wang, Z., Pane, V.E., Criddle, C.S., 2020. Metabolic model of nitrite reduction to nitrous oxide coupled to alternating consumption and storage of glycogen and polyhydroxyalkanoate. Bioresour. Technol. Reports 9, 100370. https://doi.org/10.1016/J.BITEB.2019.100370.

Wei, W., Isobe, K., Nishizawa, T., Zhu, L., Shiratori, Y., Ohte, N., Koba, K., Otsuka, S., Senoo, K., 2015. Higher diversity and abundance of denitrifying microorganisms in environments than considered previously. ISME J. 9, 1954–1965. https://doi.org/10.1038/ismej.2015.9.

Weißbach, M., Criddle, C.S., Drewes, J.E., Koch, K., 2017. A proposed nomenclature for biological processes that remove nitrogen. Environ. Sci. Water Res. Technol. 3, 10–17. https://doi.org/10.1039/C6EW00216A.

Weißbach, M., Gossler, F., Drewes, J.E., Koch, K., 2018a. Separation of nitrous oxide from aqueous solutions applying a micro porous hollow fiber membrane contactor for energy recovery. Separ. Purif. Technol. 195, 271–280. https://doi.org/10.1016/j.seppur.2017.12.016.

Weißbach, M., Thiel, P., Drewes, J.E., Koch, K., 2018b. Nitrogen removal and intentional nitrous oxide production from reject water in a coupled nitritation/nitrous denitritation system under real feed-stream conditions. Bioresour. Technol. 255, 58–66. https://doi.org/10.1016/j.biortech.2018.01.080.

Woo, S.-G., 2017. Nitrous Oxide Production in Coupled Aerobic-Anoxic Nitrous Decomposition Operation (CANDO) Bioreactors: Microbial Community Structure and Metabolic Pathways. Stanford University.

Zeng, R.J., Yuan, Z., Keller, J.J., 2003. Enrichment of denitrifying glycogen-accumulating organisms in anaerobic/anoxic activated sludge system. Biotechnol. Bioeng. 81, 397–404. https://doi.org/10.1002/bit.10484.

Zeng, R., Yuan, Z., van Loosdrecht, M.C.M., Keller, J., 2002. Proposed modifications to metabolic model for glycogen-accumulating organisms under anaerobic conditions. Biotechnol. Bioeng. 80, 277–279. https://doi.org/10.1002/bit.10370.

Zhou, Y., Pijuan, M., Zeng, R.J., Yuan, Z., 2008. Free nitrous acid inhibition on nitrous oxide reduction by a denitrifying-enhanced biological phosphorus removal sludge. Environ. Sci. Technol. 42, 8260–8265. https://doi.org/10.1021/es800650j.

Zuo, Z., Sun, L., Wang, X., Qiu, T., Han, M., Gao, J., Zhang, L., Gao, M., 2015. *Diaphorobacter polyhydroxybutyrativorans* sp. nov., a novel poly(3-hydroxybutyrate-co-3-hydroxyvalerate)-degrading bacterium isolated from biofilms. Int. J. Syst. Evol. Microbiol. 65, 2913–2918. https://doi.org/10.1099/ijs.0.000353.